The synergy of heavy-ion irradiation and lithium-lead corrosion on deuterium permeation behavior of ceramic coating
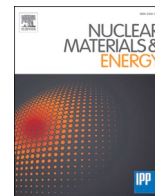
メタデータ	言語: en
	出版者: Elsevier
	公開日: 2022-02-24
	キーワード (Ja):
	キーワード (En):
	作成者: Miura, Sota, Nakamura, Kazuki, Akahoshi, Erika, Yagi, Juro, Hishinuma, Yoshimitsu, Tanaka, Teruya, Chikada, Takumi
	メールアドレス:
	所属:
URL	http://hdl.handle.net/10297/00028619

The synergy of heavy-ion irradiation and lithium-lead corrosion on deuterium permeation behavior of ceramic coating

Sota Miura [a], Kazuki Nakamura [a], Erika Akahoshi [a], Juro Yagi [b], Yoshimitsu Hishinuma [c], Teruya Tanaka [c], Takumi Chikada [a,*]

[a] *Shizuoka University, 836 Ohya, Suruga-ku Shizuoka, 422-8529, Japan*
[b] *Kyoto University, Gokasho, Uji, Kyoto 611-0011, Japan*
[c] *National Institute for Fusion Science, 322-6 Oroshi, Toki, Gifu 509-5292, Japan*

ARTICLE INFO

ABSTRACT

Functional ceramic coatings have been investigated for several decades to mitigate tritium permeation through structural materials in a fusion reactor blanket. For the establishment of a liquid blanket system, the coatings require not only tritium permeation reduction but also the tolerance to irradiation damage induced by neutrons and corrosion by liquid tritium breeders. In this study, deuterium permeation measurements under exposure to liquid lithium–lead were performed for a heavy-ion-irradiated zirconium oxide coating sample to elucidate the synergy of irradiation and corrosion on hydrogen isotope permeation. The irradiated coating decreased the deuterium permeation flux under lithium–lead exposure by more than two orders of magnitude in comparison with the unirradiated one. Each activation energy of permeation and diffusion of the coating sample was larger than that of the unirradiated one at around 450 °C and decreased to the level of the unirradiated one at 600 °C. The results indicated that the voids formed by ion irradiation aggregated in grain boundaries of the coating, resulting in an increase in the energy barrier of diffusion at low temperatures and then a decrease due to the defect recovery at high temperatures. Besides, a corrosion product layer formed on the coating during lithium–lead exposure increased the energy barrier of solution. The synergy of irradiation and corrosion on permeation was developed at lower temperatures before the defect recovery.

Introduction

A strict control of tritium is a crucial issue to establish an efficient fuel system in fusion reactors because hydrogen isotopes have high permeabilities in most metals in the operating temperature range. To reduce tritium permeation and leakage through structural materials, tritium permeation barrier (TPB) coating has been developed for several decades [1–3]. Our previous studies revealed that the ceramic coatings such as erbium oxide (Er_2O_3), yttrium oxide (Y_2O_3), and zirconium oxide (ZrO_2) coatings delivered high permeation reduction performance.

In a liquid blanket system aiming at high thermal efficiency, a TPB coating will be exposed to high-energy neutrons and gamma rays as well as high-temperature liquid tritium breeders. High-energy neutrons introduce severe damages to the coating through nuclear reactions and displacement of the crystal atoms. Heavy-ion irradiation to the coatings was previously conducted to simulate neutron damages and formed

voids, an amorphous layer, and irradiation-induced grain growth [4–7]. Moreover, irradiation defects would decrease deuterium permeability in the coating and suppress a change in crystal structure [7]. Regarding corrosion effects by liquid tritium breeders, the exposure tests to liquid lithium lead (Li-Pb) for a few kinds of ceramic coatings were performed, and ZrO_2 coatings showed high compatibility with Li-Pb [8–11].

In the context of research and development of the TPB coatings, the current focus is the elucidation of combined effects among corrosion, irradiation, and permeation. Li-Pb exposure tests for irradiated-ZrO_2-coated samples indicated an increase in the formation of corrosion products and a decrease in coating thickness in comparison with an unirradiated sample [12]. In addition, void agglomeration in grain boundaries of the coating was observed after Li-Pb exposure, indicating that the corrosion behavior would be affected by the defects. On the other hand, deuterium permeation measurements for the coatings with exposure to liquid Li-Pb were conducted to elucidate corrosion effects on the permeation behavior [13]. Degradation of the coating was detected

---

by an increase in deuterium permeation flux, while degradation of the ZrO_2 coating was restrained, suggesting that liquid Li-Pb had a possibility to change the permeation behavior. However, the coating must reduce tritium permeation with maintaining irradiation and corrosion tolerance in the actual reactor where the permeation, irradiation, and corrosion arise simultaneously. Therefore, the goal of this study is to elucidate the synergy of irradiation and corrosion on hydrogen isotope permeation.

Experimental details

Sample preparation

Reduced activation ferritic/martensitic steel F82H (Fe-8Cr-2 W, F82H-BA07 heat) plate with dimensions of 25 mm in length and 0.5 mm in thickness was used as substrate. Before fabricating a coating, the substrate was heat-treated in a quartz tube for 10 min at 710 °C in argon and hydrogen mixture gas flow with each flow rate of 50 standard cubic centimeters per minute (sccm) by reference to our previous study [10]. This treatment aimed to form a chromium oxide (Cr_2O_3) layer on the substrate for suppression of the formation of iron oxide which degrades adhesion between the coating and the substrate [14]. A ZrO_2 coating was fabricated by metal organic decomposition (MOD) using a liquid precursor (SYM-ZR-04®, Kojundo Chemical Laboratory Co., Ltd.). The MOD process is described in detail in Ref. [11], and the number of dipping, drying, pre-heating, and heat-treatment processes was followed by Ref. [12]. The thickness of the ZrO_2 coating was approximately 700 nm. The MOD process contained carbon impurity in the coatings derived from the organic precursor with an atomic concentration of up to 15 % [15].

Ion irradiation

6.0 MeV Ni^{2+} irradiation was conducted using a 3 MV tandem accelerator at Takasaki Ion Accelerators for Advanced Research Application (TIARA) in National Institutes for Quantum and Radiological Science and Technology (QST). The irradiation experiment was performed without sample heating. The Ni^{2+} beam fluence of 1.2×10^{20} m^{-2} uniformly hit on the whole surface of the coated sample.

Fig. 1 shows a depth profile of irradiation damage concentration simulated by SRIM-2013 [16] with the calculation type of full damage cascades. The threshold displacement energies of Zr, O, and Fe were set at 25, 28, and 25 eV, respectively. The estimated displacement damage concentration in the coating was 4.0 dpa. The damage density was uniform in the coating with the Bragg peak in the substrate, indicating

Fig. 1. Depth distributions of damage concentration and Ni concentration calculated by SRIM-2013.

that the irradiation condition nicely simulated a damage distribution in the coating brought by high-energy neutron irradiation.

Deuterium permeation measurement with exposure to liquid Li-Pb

Deuterium permeation measurements under liquid Li-Pb exposure condition is described in detail in Ref. [13]. Before mounting the sample to a pair of sample holders, the backside of the sample was polished with abrasive papers to remove an oxide layer of the substrate and residual MOD precursor. A palladium coating was deposited on the surface of the bare substrate by radio-frequency magnetron sputtering to prevent the formation of oxide layers during the permeation measurements. Thereafter, the sample was placed in the apparatus with the coated side facing to the upstream, and liquid Li-Pb was introduced into the upstream. Li-Pb was synthesized from Li (purity: 99.9 %) and Pb (purity: 99.9 %) purchased from Furuuchi Chemical Co. with an atomic ratio of 15.7:84.3 under argon atmosphere in a glove box. The amount of introduced Li-Pb was approximately 9.2 g corresponding to 1.0 cm in thickness in the permeation device to cover the whole sample surface.

The procedure of the permeation experiments was followed by Ref. [17]. The deuterium permeation flux through the Li-Pb and the ZrO_2-coated sample was detected using a quadrupole mass spectrometer (QMS) with the driving pressure of 10.0–80.0 kPa. Ion currents of $m/z = 3$ and 4 corresponding to HD and D_2 were calibrated using a deuterium standard leak. The sample temperature was 250–600 °C, and the tests were started from lower temperatures. Finally, the permeation flux was monitored for 300 h at 600 °C with the deuterium driving pressure of 80 kPa to investigate thermal durability of the coating.

The deuterium permeation flux J through the substances expressed by the following equation:

$$J = K_S D \frac{p^n}{d} \tag{1}$$

where K_S is Sieverts' constant, D is the diffusivity, p is the driving pressure, and d is the thickness of the sample. In this study, the thickness of Li-Pb did not include in d based on an assumption that deuterium permeation is mainly dominated by the coated sample in this system. The pressure exponent n was obtained by the permeation fluxes with different driving pressures at each temperature. The simplest case of permeation, where the rate-limiting step is a deuterium atom process such as solution and diffusion, satisfies the equation with $n = 0.5$. When the permeation rate is limited by a molecular process such as adsorption and desorption, the exponent of the driving pressure p is unity ($n = 1$). The diffusivity D is calculated using a time lag t_{lag} for the permeation flux to reach a steady state by the following equation [18]:

$$t_{lag} = \frac{d^2}{6D}. \tag{2}$$

Due to a significantly low diffusivity of ZrO_2 in comparison with Li-Pb, the calculated diffusivity mainly reflects the ZrO_2-coated sample and the corresponding corrosion product layer. In addition, the activation energies of deuterium permeation E_P and diffusion E_D were estimated by fitting a gradient of temperature dependence of the permeation flux and the diffusivity because each process is a thermally-activated process [17]. The relationship between E_P and E_D is expressed by the following equation [19,20]:

$$E_P = E_D + \Delta H_S, \tag{3}$$

where ΔH_S is the enthalpy difference of solution between the gaseous state and the sample. A schematic illustration of the permeation model is shown in Fig. 2. Although each layer has energy barriers of deuterium solution and diffusion, the total enthalpy difference between gas to ZrO_2 and a sum of diffusion barrier in Li-Pb, the corrosion product layer, and ZrO_2 coating were obtained in the permeation measurements.
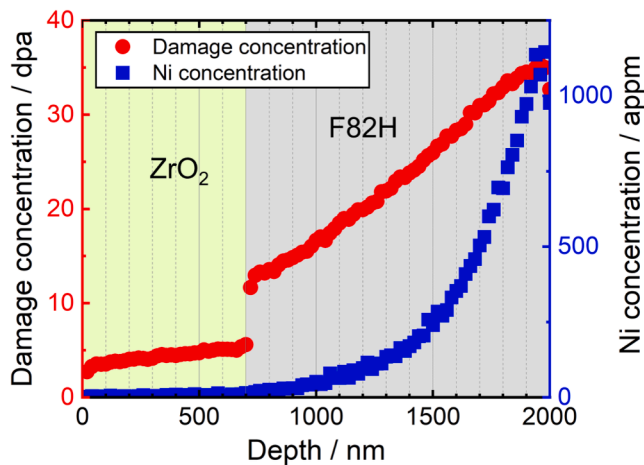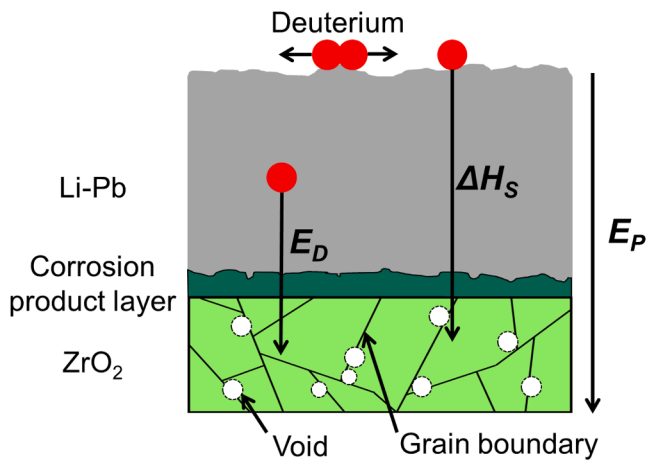
Fig. 2. Conceptual diagram of enthalpy difference and energy barriers for deuterium permeation through liquid Li-Pb and irradiated ZrO_2 coating.

Characterization

After the permeation tests, the Li-Pb introduced in the upstream was removed by heating, and the sample was shaken out to remove the adhering Li-Pb in a glove box. We did not chemically remove Li-Pb to avoid damage to the sample during cleaning. Surface observations and chemical analyses were conducted by a field emission scanning electron microscope (FE-SEM, JSM- 7100F, JEOL Ltd.) with energy dispersive X-ray spectroscopy (EDX). To estimate free energies for formation and melting points of the Li compounds, the thermodynamic database Materials-oriented Little Thermodynamic database (MALT) [21] was used.

Results

Deuterium permeation flux

Fig. 3 shows the temperature dependence of the deuterium permeation flux for the ZrO_2-coated sample. Calculated activation energies of permeation E_P for uncoated F82H, unirradiated ZrO_2 coating from previous data [13], and Ni^{2+}-irradiated ZrO_2 coating with Li-Pb were also indicated. The permeation fluxes in the first measurements at 250 and 300 °C were relatively high probably due to insufficient crystallization of the coating through the MOD process and the irradiation. In the test at 450 °C, the flux decreased by a factor of 13,000 in comparison with that of the uncoated F82H substrate. The high permeation reduction was the largest in the previous ZrO_2-coated samples [10,13]. At 450–550 °C, the fluxes steeply increased with temperature, and calculated E_P was 182 kJ mol^{-1} which was three times as large as that of the ZrO_2-coated sample. After the measurement at 550 °C, the flux at 400 °C showed a value similar to that of the first test. Estimated E_P was 41 kJ mol^{-1} from these two values at 550 and 400 °C. The fluxes in subsequent tests at 600, 500, 450, and 400 °C decreased with temperature, and calculated E_P was 68 kJ mol^{-1}. The E_P value was similar to that of the unirradiated-ZrO_2-coated sample (60 kJ mol^{-1}). Regarding the rate-limiting process of permeation, the pressure exponent n in the measurements at 250–400 °C showed values larger than 0.5, indicating a contribution of surface reactions. The value gradually increased to 1.0 with increasing temperature in the measurements more than 400 °C, while dropped to 0.5 at 550 °C. Fig. 4 shows a temporal change of permeation fluxes in the test at 600 °C after the above-mentioned tests. During the test for approximately 300 h, the deviation of the flux was within 10 %, which proves a soundness of the coating at elevated temperature.

Diffusivity

Fig. 5 shows the temperature dependence of the diffusivity in the ZrO_2 coating and the activation energies of diffusion E_D calculated from the present data and the previous study [13]. E_D of unirradiated ZrO_2 was calculated using the data at only less than 500 °C because no diffusivity data were available at 500 °C and higher temperatures. In the tests of the present study at less than 400 °C, the diffusivities were relatively high as well as the permeation fluxes shown in Fig. 3. At 400–500 °C, the diffusivities increased with temperature, and the calculated E_D was 59 kJ mol^{-1} which was a higher value than that of F82H and unirradiated-ZrO_2-coated sample with Li-Pb. Thereafter, the diffusivity decreased at 550 °C and then showed a value in the second test at 400 °C similar to the first one. The estimated E_D from the two values at 550 and 400 °C was 48 kJ mol^{-1}. E_D was always lower than E_P, and the trend of the diffusivity and E_D did not correspond to the permeation flux and E_P. After that, the diffusivity in the test at 600 °C was less than that at 550 °C. The estimated E_D from the data in subsequent tests at 500, 450, and 400 °C was 25 kJ mol^{-1}, although these data did not lie on a straight line. This low value was similar to that of unirradiated ZrO_2 coating with Li-Pb as well as F82H.
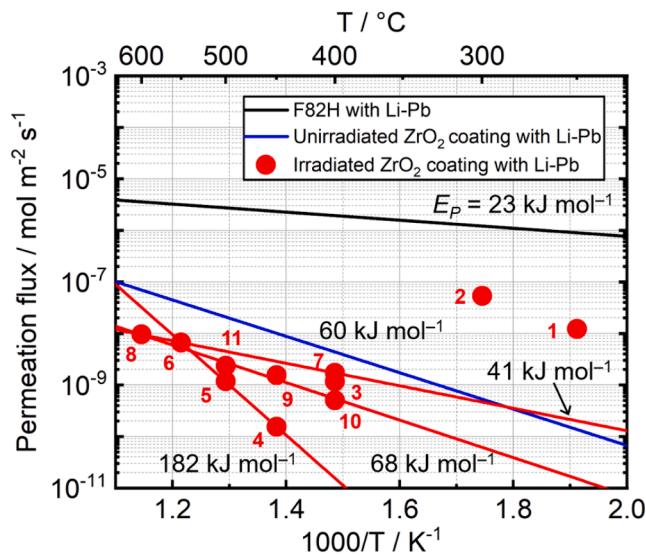

Fig. 3. Arrhenius plots of deuterium permeation flux for F82H substrate and ZrO_2-coated sample with Li-Pb. Numbers next to symbols represent test sequence.
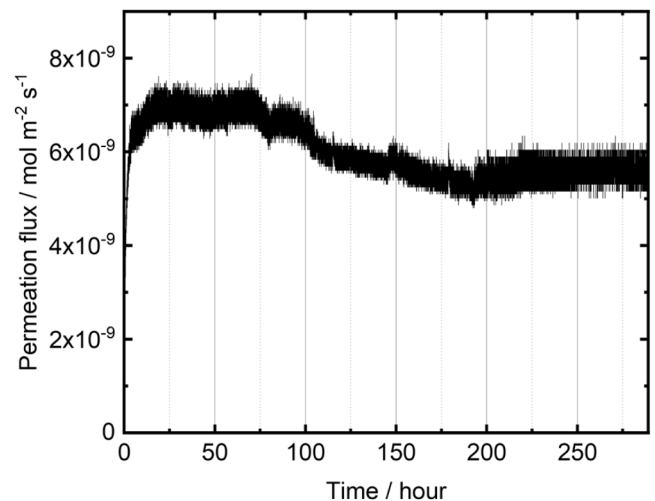

Fig. 4. Temporal change of deuterium permeation flux in permeation test with exposure to Li-Pb at 600 °C.
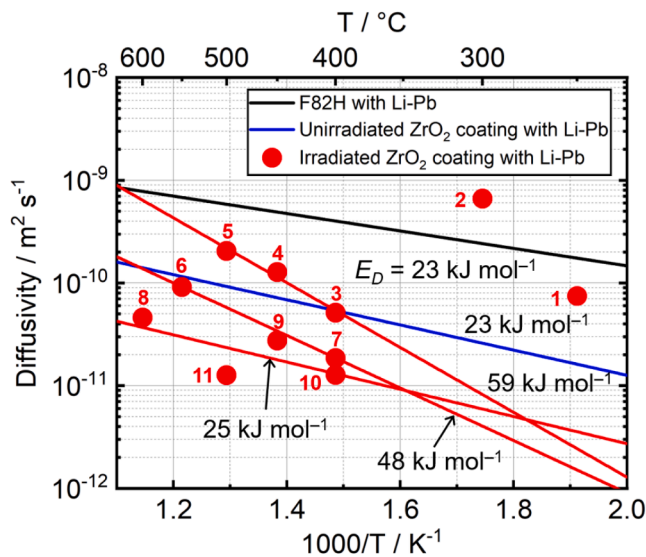
Fig. 5. Arrhenius plots of diffusivity for F82H substrate and ZrO$_2$-coated sample with Li-Pb. Numbers next to symbols represent test sequence.

Surface analysis

Surface SEM images of the irradiated ZrO$_2$ coating after the permeation tests with exposure to Li-Pb are shown in Fig. 6 with different magnifications. In addition to the ZrO$_2$ coating and Li-Pb, another layer formed on the coating. No crack and peeling were generated in the coating, which is consistent with the quite low permeation fluxes. On the other hand, the layer formed on the coating cracked and peeled everywhere. EDX results indicated that atomic concentrations of carbon in the coating and the layer were approximately 8 and 16 %, respectively; therefore, the layer might consist of corrosion products due to a large concentration of carbon [11].

Discussion

Corrosion product

The formation of the corrosion product layer was confirmed on the irradiated ZrO$_2$ coating after Li-Pb exposure, and its thickness was smaller than that of the ZrO$_2$ coating [12]. The layer structure in this study might be same as those in the reference because the exposure temperature and duration were quite similar. In this case, the inconsistency in the trends between the permeation flux and the diffusivity when the temperature changed from 400 °C to 450 °C, 500 °C to 550 °C, and 550 °C to 600 °C can be explained with a few speculations. Since the permeation consists of solution and diffusion, the inconsistency between permeation and diffusion should be attributed to a change in solution behavior. Then, the most probable reason of the decrease in only the

permeation flux from 400 °C to 450 °C (the measurement number of 3 and 4) would be the formation of the corrosion product layer. The diffusivity did not decrease from 400 °C to 450 °C and increase linearly up to 500 °C, which indicates the contribution of the corrosion product layer to diffusion is small. It should be also noted that the inside of liquid Li-Pb would be another factor of contribution to the permeation. Because the thickness of the introduced liquid Li-Pb was 20 times larger than the coated sample, Li-Pb had some effects on the permeation even if the deuterium diffusivity in Li-Pb is significantly higher than that in the sample.

Fig. 7 shows free energies of formation of the supposed Li compounds calculated by MALT. Although some reactions could progress in this study, Li$_2$CO$_3$ and Li$_2$ZrO$_3$ would form on the ZrO$_2$ coating because Li$_2$CO$_3$ is the most thermodynamically formable, and the formation of Li$_2$ZrO$_3$ was confirmed in the previous study [13]. These compound layers might increase the energy barrier of solution, resulting in the low permeation flux at 450 °C. Besides, the formation of other corrosion products on the Li-Pb and dissolution in the Li-Pb might be associated with the increase in values of the pressure exponent n at low temperature during the permeation test. The SEM images showed cracks and peelings of the corrosion product layer; however, it is highly possible that the degradation of the layer occurred after the series of the permeation tests due to the fact that no rapid changes in the permeation flux were detected throughout the measurements. Additionally, unlike our previous study [12], a decrease in coating thickness and an increase in the amount of corrosion products after Li-Pb exposure test were not confirmed through the permeation tests, indicating that the effects of the layer on the deuterium diffusion and solution behaviors were precisely investigated under the experimental condition in this study.
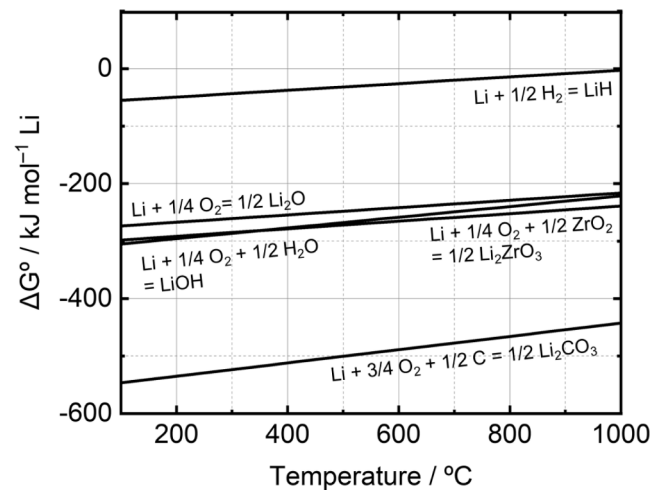

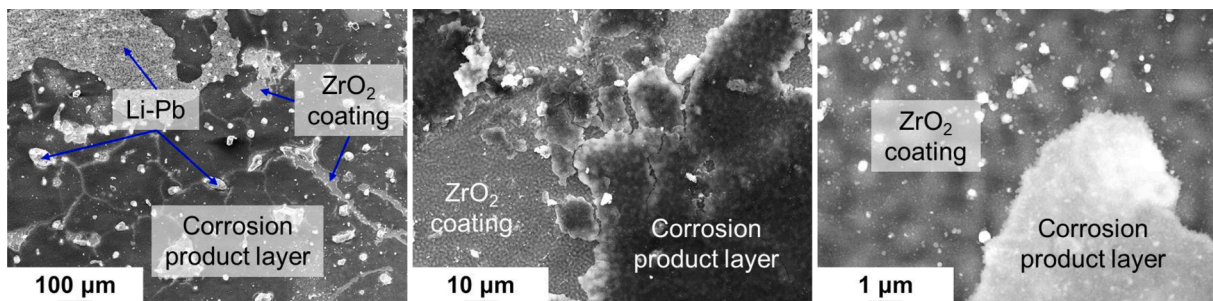**Fig. 7.** Free energies of formation of the Li compounds calculated by MALT.

Fig. 6. Surface SEM images of irradiated-ZrO$_2$-coated sample after permeation with exposure to Li-Pb.

Irradiation effect

As mentioned in the previous section, the corrosion products would affect the solution the most. In other words, the diffusion is supposed to be mainly affected not by surface but by inside structure of the irradiated ZrO_2 coating. According to Fig. 5, the calculated E_D in the temperature range of 400–500 °C was the highest in the other samples with Li-Pb (59 kJ mol^{-1}), indicating the largest energy barrier of diffusion in the irradiated sample. In the previous studies, it was revealed that deuterium permeation in a ceramic coating was dominated by grain boundary diffusion [23], and voids generated by heavy-ion irradiation were accumulated in grain boundaries [12,22]. Therefore, it is highly possible that the voids accumulated in the grain boundaries of the ZrO_2 coating increased the energy barrier of diffusion.

On the other hand, the decrease in E_D after the tests at 550 and 600 °C would be ascribed to the elimination of irradiation effect. One reason is recovery of the voids. Our previous study indicated that the voids in the irradiated Y_2O_3 coating suppressed the permeation only at low temperatures (less than500 °C) and were annihilated at high temperatures [7]. The same phenomenon might occur in the ZrO_2 coating. Also, it was suggested that the permeation was restrained by the voids before the test at 600 °C, and the defect recovery occurred at this temperature. The other reason is the movement of the voids to sites where deuterium diffusion is not affected. In the high temperatures, not only thermal energy but also larger deuterium flux would increase the mobility of the voids.

Synergy of corrosion and irradiation

From the above discussions, we consider that the corrosion product layer and the void agglomeration in grain boundaries would affect solution and diffusion, respectively. In that sense, the effects of corrosion and irradiation on deuterium permeation were separately investigated in this study. In addition, the synergy of corrosion and irradiation would be shown only before conducting the permeation test at 550 °C since the permeation behavior became similar to the unirradiated-ZrO_2-coated sample after the test at high temperatures. In the actual reactor, the coating will be exposed to irradiation and corrosion simultaneously, which causes a different synergy effect from this study. At the beginning of reactor operation, the corrosion effect would be dominant since the damage rate by neutron irradiation is much smaller than ion irradiation using accelerators. Moreover, the irradiation damage will easily recover under operation temperature, which is also a different condition from this study. However, the situation is rather simple because irradiation effects is negligibly small. As the operation time is accumulated, the agglomeration of irradiation defects gradually occurs, and the accumulated irradiation damage will affect the corrosion behavior as discussed in this study. It should be noted that the degradation of the ZrO_2 coating may occur under a test condition severer than this study, leading to a significant increase of the permeation flux.

Further analysis of irradiated samples after the permeation tests with exposure to Li-Pb were needed for a precise understanding of the synergy of irradiation and corrosion on the permeation behavior. The maximum test temperature is also important to control the formation and solution of Li compounds and irradiation damage in the coating.

Conclusions

Deuterium permeation behavior with exposure to Li-Pb for the Ni^{2+}-irradiated ZrO_2 coating sample was investigated. Each activation energy of permeation and diffusion calculated at around 450 °C was larger than that of the unirradiated one and decreased to the level of the unirradiated one at 600 °C. The agglomeration of the voids in grain boundaries of the coating would increase the energy barrier of diffusion at low temperatures, while the defects were recovered at high temperatures. In addition, the permeation fluxes were lower than that of the unirradiated

one in the test temperature range. The permeation flux decreased by a factor of 13,000 compared to that of the F82H sample at 450 °C probably because the corrosion product layer increased the energy barrier of solution. The corrosion product layer and the voids would synergistically affect the permeation behavior at low temperatures. The effects of irradiation and corrosion could be separated into diffusion and solution, respectively.

CRediT authorship contribution statement

Sota Miura: Conceptualization, Methodology, Investigation, Resources, Writing – original draft. **Kazuki Nakamura:** Investigation, Resources. **Erika Akahoshi:** Investigation, Resources. **Juro Yagi:** Investigation, Resources. **Yoshimitsu Hishinuma:** Investigation, Resources. **Teruya Tanaka:** Investigation, Resources. **Takumi Chikada:** Conceptualization, Methodology, Investigation, Resources, Writing – review & editing, Supervision, Project administration, Funding acquisition.

Declaration of Competing Interest

The authors declare that they have no known competing financial interests or personal relationships that could have appeared to influence the work reported in this paper.

References

[1] G.W. Hollenberg, et al., Tritium/hydrogen barrier development, Fusion Eng. Des. 28 (1995) 190–208.
[2] J. Konys, et al., Status of tritium permeation barrier development in the EU, Fusion Sci. Technol. 47 (4) (2005) 844–850.
[3] T. Chikada, Ceramic coatings for fusion reactors, in: R. Konings, R. Stoller (Eds.), Comprehensive Nuclear Materials, 2nd edition, Elsevier, Oxford, 2020, pp. 274–283.
[4] Y. Hishinuma, et al., Microstructure and peeling behavior of MOCVD processed oxide insulator coating before and after ion beam irradiation, Nucl. Mater. Energy 16 (2018) 123–127.
[5] F. García Ferré, et al., Extreme ion irradiation of oxide nanoceramics: influence of the irradiation spectrum, Acta Mater 143 (2018) 156–165.
[6] K. Nakamura, et al., Iron-ion irradiation effects on microstructure of yttrium oxide coating fabricated by magnetron sputtering, Fusion Eng. Des. 146 (2019) 2031–2035.
[7] K. Nakamura, et al., Effects of helium implantation with heavy ion irradiation on deuterium permeation in yttrium oxide coating, J. Nucl. Mater. 537 (2020), 152244.
[8] T. Chikada, et al., Fabrication technology development and characterization of tritium permeation barriers by a liquid phase method, Fusion Eng. Des. 136 (2018) 215–218.
[9] M. Matsunaga, et al., Lithium-lead corrosion behavior of erbium oxide, yttrium oxide and zirconium oxide coatings fabricated by metal organic decomposition, J. Nucl. Mater. 511 (2018) 537–543.
[10] J. Mochizuki, et al., Preparation and characterization of Er_2O_3-ZrO_2 multi-layer coating for tritium permeation barrier by metal organic decomposition, Fusion Eng. Des. 136 (2018) 219–222.
[11] E. Akahoshi, et al., Corrosion tests of multi-layer ceramic coatings in liquid lithium-lead, Fusion Eng. Des. 160 (2020) 111874.
[12] S. Miura, et al., Lithium-lead corrosion behavior of zirconium oxide coating after heavy-ion irradiation, Fusion Eng. Des. 170 (2021) 112536.
[13] E. Akahoshi, et al., Deuterium permeation through multi-layer ceramic coatings under liquid lithium-lead exposure condition, Corros. Sci. 189 (2021), 109583.
[14] T. Tanaka, T. Muroga, Control of substrate oxidation in MOD ceramic coating on low activation ferritic steel with reduced-pressure atmosphere, J. Nucl. Mater. 455 (1-3) (2014) 630–634.
[15] S. Nakazawa, et al., Gamma-ray irradiation effect on deuterium retention in reduced activation ferritic/martensitic steel and ceramic coatings, J. Nucl. Mater. 539 (2020), 152321.
[16] http://srim.org.
[17] T. Chikada, et al., Surface behaviour in deuterium permeation through erbium oxide coatings, Nucl. Fusion 51 (2011), 063023.

[18] J. Crank, The Mathematics of Diffusion, second ed., Clarendon Press, Oxford, UK, 1975.

[19] T. Chikada, et al., Deuterium permeation behavior in iron-irradiated erbium oxide coating, Fusion Eng. Des. 124 (2017) 915–918.

[20] E. Serra, et al., Influence of traps on the deuterium behavior in the low activation martensitic steels F82H and Batman, J. Nucl. Mater. 245 (1997) 108–114.

[21] H. Yokokawa, et al., Thermodynamic database MALT for windows with gem and CHD, Calphad 26 (2) (2002) 155–166.

[22] X.-M. Bai, et al., Efficient annealing of radiation damage near grain boundaries via interstitial emission, Science 327 (2010) 26.

[23] T. Chikada, et al., Microstructure change and deuterium permeation behavior of erbium oxide coating, J. Nucl. Mater. 417 (1–3) (2011) 1241–1244.